Thermo-mechanical modelling of additive manufacturing: activation of non-constructed domain and effect of kinematic hardening

Joël Keumo Tematio, L Ravix, Y Zhang, Michel Bellet

Thermo-mechanical modelling of additive manufacturing: activation of non-constructed domain and effect of kinematic hardening

Thermo-mechanical modelling of additive manufacturing: activation of non-constructed domain and effect of kinematic hardening

J Keumo Tematio, L Ravix, Y Zhang*, M Bellet

Mines Paris, PSL University, CEMEF – Centre de Mise en Forme des Matériaux, CNRS UMR 7635, Sophia Antipolis, France. *E-mail: yancheng.zhang@minesparis.psl.eu

Abstract. A thermo-mechanical finite element model is developed for additive manufacturing by directed energy deposition (DED). The simulation is conducted at the part scale by modelling the progressive deposition in the way of the fraction of the layer. To incrementally resolve the displacement, strain, and stress fields, a theoretical formulation for the kinematic positioning is proposed to minimize the distortion of the non-constructed fraction by considering current displacement and strain in the constructed part, which can resolve the discontinuous problem at the interface for a patch of material depositions. Moreover, it is found that the kinematic hardening couldn't be ignored for the back-and-forth deposition mode of the DED process. The application for a turbine blade with a strong curvature is adopted, and the distributions of distortion and stress during mid-construction and final construction are studied.

1. Introduction

Among different additive manufacturing (AM) processes, directed energy deposition (DED) is widely adopted due to its efficiency, flexibility, and construction possibility of near-net-shape [1]. However, expensive and time-consuming experimental work is still needed to find the optimized parameters for the new structures and new materials. Recently, numerical simulation of DED processes has received great interest, especially with developments of computational resources and numerical techniques. To access the evolution of the part during its construction, such as distortions and stress, macro-scale thermo-mechanical numerical simulations are usually proposed.

In the available models, the quiet element method, inactive element method, and hybrid inactive/quiet element method are usually adopted to deal with the non-activated domain. Then two questions are posed: how to deal with the physical information consisting of thermal and mechanical aspects at the interface between the active and inactive (or quiet) elements? which type of material constitutive law should be adopted to simulate back-and-forth deposition mode?

Once the elements in the non-construction domain are activated, the physical information of the interface should be carefully handled. Regarding the thermal aspect, Michaleris [2] gives detailed discussions on numerical treatments of the quiet element method and inactive element method. No special treatment is needed for the quiet element method, but the scaling factors for the thermal conductivity and specific heat should be carefully verified to avoid artificial energy input. For the inactive element method, the activated

elements and their nodes shared by active elements may not be at the initial temperature, which can result in artificial energy input, so resetting the new activated elements to the initial temperature for the numerical solver resolution is required.

However, from the mechanical point of view, few articles give detailed information on the element activation of the non-activated domain. For the method of the quiet element, the initial distortion existed for the new active elements by considering a small Young's modulus in the non-activated domain, the different magnitude of a small Young's modulus may lead to different modes of distortion as presented in the work of Biegler *et al*. [3]. For the method of inactive element (Baiges *et al*. [4]), the initial displacement field of the newly activated elements is induced by the nodes shared with the pre-existing active elements, and the inherited initial strain obtained by the initial displacement is removed from the following stress computation. Continuous displacement can be obtained by the above treatment, while the discontinuities of strain or stress may happen for activating a patch of elements.

Additive manufacturing is a high temperature accompanied process, the reasonable material laws at high temperatures and low temperatures should be adopted to simulate the process simulation, especially for a big number of layer depositions and long dwell time. Most of the numerical models employ the elastoplastic law with strain hardening or without strain hardening (Biegler *et al*. [3]). The elasto-viscoplastic law is also adopted by Zhang *et al*. [5], in which the viscoplastic flow rule is adopted for the solid and semi-solid states, and an incompressible Newtonian constitutive model is applied for the liquid state. Similarly, elasto-viscoplastic law is proposed by Stender *et al*. [6] for the solid and semi-solid states. Moreover, a recrystallization effect and static recovery are modeled. However, the kinematic hardening has not been yet considered, it may be a key factor in the accurate prediction of stress and strain, especially for the back-and-forth deposition mode of the DED process.

In this work, a fraction of layer-based thermo-mechanical finite element simulation is developed for DED additive manufacturing by inactive element method, where a theoretical formulation for the kinematic positioning is proposed to minimize the distortion of the non-constructed fraction by considering the current displacement and strain of the interface shared elements in the active constructed part. Simulation results of the proposed inactive element method are compared with those of the quiet element method. Moreover, it is found that it's essential to consider kinematic hardening for stress prediction in the back-and-forth deposition of the DED process.

2. Quasi-static mechanical analysis

Under the hypothesis of small deformation, the static equilibrium and mass conservation are resolved for the FE resolution by equation (1).

$$\begin{cases} \boldsymbol{\nabla \cdot \sigma} & = & \mathbf{0} \\ \boldsymbol{\nabla \cdot v} + \dfrac{\dot{p}}{\chi_b} - 3\alpha\dot{T} & = & 0 \end{cases} \tag{1}$$

where $\boldsymbol{\sigma}$ is the stress tensor, p is the pressure equal to $(-\frac{1}{3})tr\boldsymbol{\sigma}$ and $\chi_b = \frac{E}{3(1-2v)}$ is the bulk elastic modulus., α is the linear thermal expansion coefficient, and $\dot{T}$ is the temperature rate.

One main objective of this paper is to propose a thermo-elastic-viscoplastic (EVP) constitutive model considering the isotropic and kinematic hardening. The general formulations of the EVP constitutive equations are given below:

$$\dot{\boldsymbol{\varepsilon}} = \dot{\boldsymbol{\varepsilon}}^{el} + \dot{\boldsymbol{\varepsilon}}^{vp} + \dot{\boldsymbol{\varepsilon}}^{th} \tag{2}$$

$$\dot{\boldsymbol{\varepsilon}}^{el} = \left(\mathbf{D}^{el}\right)^{-1}\dot{\boldsymbol{\sigma}} = \frac{1+\upsilon}{E}\dot{\boldsymbol{\sigma}} - \frac{\upsilon}{E}\mathrm{tr}(\dot{\boldsymbol{\sigma}})\mathbf{I} \tag{3}$$

$$\dot{\boldsymbol{\varepsilon}}^{th} = \alpha\dot{T}\mathbf{I} \tag{4}$$

$$\dot{\boldsymbol{\varepsilon}}^{vp} = \frac{3}{2\bar{\sigma}}\left[\frac{\bar{\sigma}(\mathbf{s}-\mathbf{X}) - (\sigma_Y + R(\bar{\varepsilon}))}{K_{vp}}\right]_+^{1/m}(\mathbf{s}-\mathbf{X}) \tag{5}$$

where the strain rate tensor $\dot{\boldsymbol{\varepsilon}}$ (equation (2)) is split into an elastic part, $\dot{\boldsymbol{\varepsilon}}^{el}$, a viscoplastic part, $\dot{\boldsymbol{\varepsilon}}^{vp}$, and a thermal part, $\dot{\boldsymbol{\varepsilon}}^{th}$. The latter consists of the thermal expansion rate (equation (4)), with α the one-dimensional thermal dilation coefficient. Equation (3) is the hypo-elastic Hooke's law where E denotes Young's modulus, and υ the Poisson's coefficient. $\dot{\boldsymbol{\sigma}}$ denotes the total time derivative of the stress tensor. Finally, equation (5) expresses the relation between the viscoplastic strain-rate tensor and the stress deviator $\mathbf{s}$ and back stress $\mathbf{X}$. Coefficient K_{vp} is the viscoplastic consistency, σ_Y denotes the initial yield stress. The function $[x]_+$ is equal to 0 when x is negative and to x otherwise. Coefficient m is the strain-rate sensitivity, and the strain hardening function R depends on the equivalent plastic strain $\bar{\varepsilon}$ which is the time-integral of the generalized strain-rate $\dot{\bar{\varepsilon}}$. From equation (5), when $\dot{\boldsymbol{\varepsilon}}^{vp} \neq \mathbf{0}$, and calculating $\dot{\bar{\varepsilon}}$, the following scalar relation can be easily obtained:

$$\bar{\sigma} = \sigma_Y + R(\bar{\varepsilon}) + k\dot{\bar{\varepsilon}}^m \tag{6}$$

Consequently, equation (5) can be straightforwardly rewritten:

$$\dot{\boldsymbol{\varepsilon}}^{vp} = \frac{3\dot{\bar{\varepsilon}}}{2\bar{\sigma}}(\mathbf{s}-\mathbf{X}) \tag{7}$$

Similar to the work of Smith *et al*. [7], the back stress $\mathbf{X}$ related to the kinematic hardening is defined as a non-linear form by ignoring the temperature and field variable dependencies.

3. Activation of the non-constructed domain

The activation of the non-constructed domain is based on the fraction of the layer along the deposited path, which contains a set of elements. The treatment of thermal aspects follows the work of Michelaris [2], which will not be elaborated on here. The main objective of this section will focus on the mechanical treatment in the following work.

Based on the inactive element method, it consists in describing the set of equations that determine the Lagrangian distortion $\boldsymbol{u}_{nb}$ related to the positioning of the non-built domain Ω_t^{nb}, which locates at t based on the built domain Ω_t. It will prepare for the deposition of a new fraction (dashed zone in **Figure 1**) at time interval $[t, t+\Delta t]$. The global principle of these equations will minimize the quantity of the initial distortions and strains within Ω_t^{nb} by equation (8), under the constraint of continuity of the global distortion $\boldsymbol{u}_t$ at the interface of activation Γ_t by equation (10), with the assumption of the incompressibility of volume by equation (9). The penalty coefficient η_p is introduced to control the weight of the minimization term of the global distortion $\boldsymbol{u}_t$, which can be determined by sensitivity analysis.

$$f\left(\boldsymbol{u}_t^{nb}\right) = \min\frac{1}{2}\int_{\Omega_t^{nb}}\left(\boldsymbol{\varepsilon}(\boldsymbol{\omega}_t):\boldsymbol{\varepsilon}(\boldsymbol{\omega}_t)+\eta_p\boldsymbol{\omega}_t:\boldsymbol{\omega}_t\right)\mathrm{dv} \tag{8}$$

$$\nabla.\boldsymbol{u}_t^{nb} = 0 \; in \; \Omega_t^{nb} \tag{9}$$

$$\boldsymbol{u}_t = \boldsymbol{u}_t^{nb} \text{ at } \Gamma_t \tag{10}$$

where $\boldsymbol{\omega}_t$ is the intermediate variable to determine $\boldsymbol{u}_t^{nb}$. The initialized distortion is based on the CAD configuration. Once the initialization step is finished, the physical deposition is performed during $[t, t+\Delta t]$ as described in section 1. The proposed method can resolve the discontinuities of deformation and strain (stress).

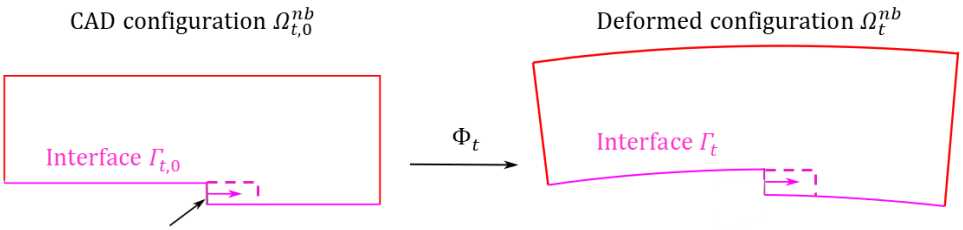

Figure 1. Initialization of no-built domain based on the CAD configuration

4. 3D Geometrical Model

In this paper, a thin-walled and curved DED geometry from the work of Biegler *et al.*[3] was chosen, as given in **Figure 2**, where the local curvilinear coordinate frame (t, n, z) is defined for demonstrating the local mechanical information (**Figure 2** (b)).

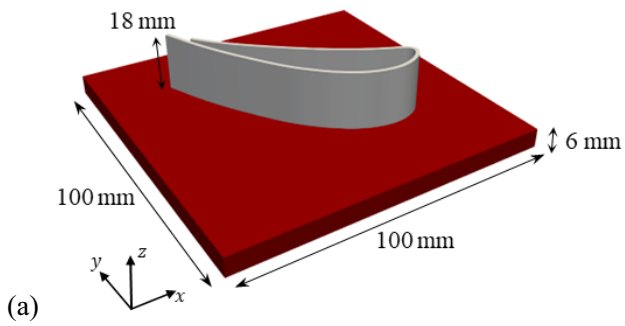

Figure 2. The geometry of the 30-layer turbine blade mock-up and defined coordinates: (a) 3D view; (b) deposition path in the horizontal plane, with the definition of global and local referential frames.

As the structure has varying curvature, high stiffness at the tip and low stiffness at the free ends, the numerical predictions of the distortion and stress will be very sensitive to different numerical methods and different material constitutive models. The same process parameters are also taken from the work of Biegler *et al.* [3], but only a regular dwell time of 30 s is considered, without the cooling break of 300s. The adopted thermal properties (Kim *et al*. [8]), the corresponding thermal boundary conditions, process parameters, and the dimension of the part are given in **Figure 2**. The non-linear thermal analysis is performed, more detailed information can be found in the PhD thesis of Keumo Tematio [9].

Table 1. Simulation data: material and process parameters, geometrical data of the turbine blade mock-up.

	Properties	**Values or reference**
Material properties (316L)	Thermophysics	Kim *et al*. [8]
	Initial temperature, T_0 [K]	298.15
	Ambient temperature, T_∞ [K]	298.15
Heat exchange	Convection coefficient, h_{conv} [W m^{-2} K^{-1}]	35
	Emissivity, ε	0.6
	Stefan–Boltzmann constant, σ [W m^{-2} K^{-4}]	5.670374×10^{-8}
	Nominal laser power, P_L [W]	400
Laser processing	Scan speed, v_L [mm s^{-1}]	10
(Biegler *et al*. [3])	Reflection coefficient, R	0.7
	Spot diameter, ϕ_L [mm]	0.6
	Curvilinear length, L [mm]	155.4
Dimension of part	Layer width, l_D [mm]	1.2
(Biegler *et al*. [3])	Layer thickness, h_D [mm]	0.6
	Total height, H [mm]	18

5. Effect of minimization of non-built domain

For the mechanical analysis, the values of plastic material properties are fitted by the work of Depradeux [10], in which only isotropic hardening is considered by the powder law $R(\bar{\varepsilon}) = H\bar{\varepsilon}^n$, where H is the hardening modulus and the n strain-hardening exponent. The elastic properties are given in Depradeux [10].

To study the method of minimization of the initial distortions and strains within the non-activated domain, a value of 0.25 is taken for the penalty coefficient η_p of the inactive element method, based on the equations (8-10). The simulation results are compared with those of the quiet element method by setting Young's modulus of 1GPa and 10GPa at mid-construction and final construction after dwell time.

5.1. During the mid-construction

Figure 3 presents the distributions of displacement (u_t) and stress (σ_{tt}) of the entire simulation domain for both inactive element method and quiet element method. The results are demonstrated at the instant close to half of the deposition of the 15th layer, at the mid-construction of the part. To better demonstrate the non-construction domain, the semi-transparent plot is adopted. By the displacement distributions, the value of u_t in the non-construction domain trends to be zero by the standard inactive element method except at interface, while non-negligible values are found for the quiet element method for both 1GPa and 10GPa of the Young's modulus in the non-construction domain. For the stress distribution of σ_{tt}, fewer differences are found for the two methods, while the σ_{tt} distribution of 1GPa is closer to that of the standard inactive element method.

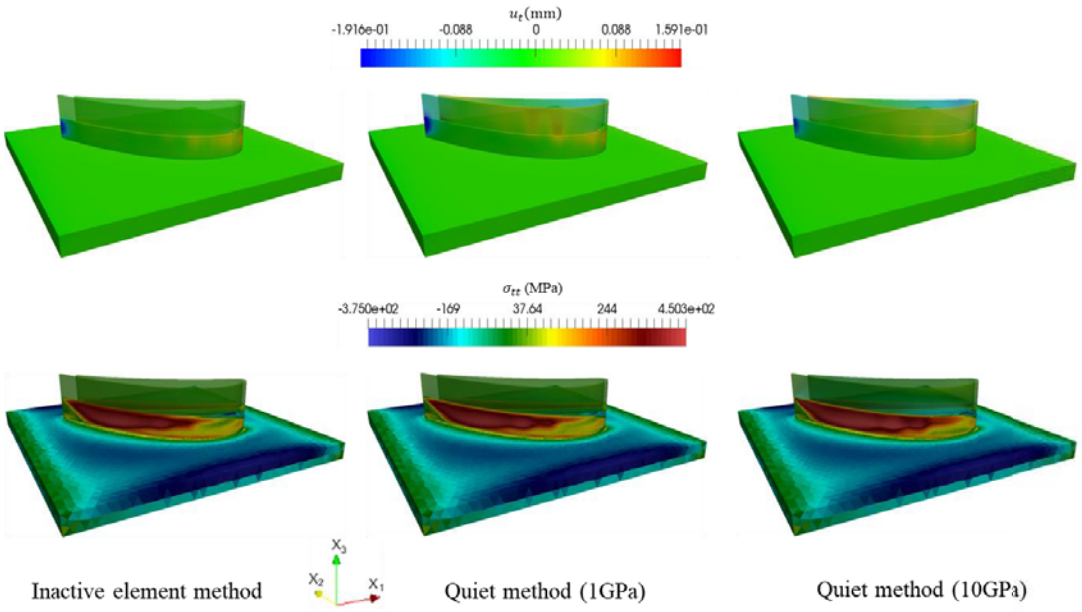

Figure 3. Displacement and stress distributions with inactive element method and quiet element method at the half deposition of the 15th layer. Construction domain: solid plot; non-construction domain: semi-transparent plot.

5.2. End of the construction

Compared with mid-construction, similar phenomena are found for both displacement and stress distribution at the end of construction. In **Figure 4**, the distortion predicted by the inactive element method lies between those estimated by the quiet element method for 1GPa and 10GPa, and the case of 1GPa overestimates the distortion and 10GPa underestimates the distortion. For the stress distribution, the two methods give similar results. Again, for the small Young's modulus, the stress distribution of 1 GPa nearly superposes with that of the inactive element method.

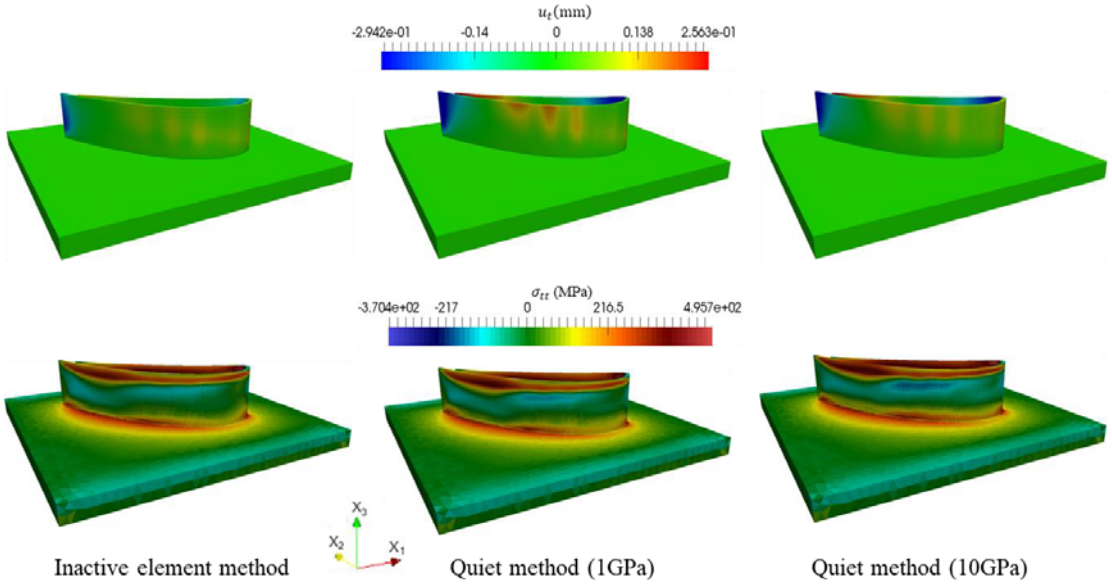

Figure 4. Displacement and stress distributions with inactive element method and quiet element method at the 30th layer.

6. Effect of kinematic hardening

To study the effect of kinematic hardening on the alternative deposition, the mixed isotropic-kinematic hardening simulation is adopted, where the material parameters of the non-linear form related to equation (6) are taken from the work of Smith *et al.* [7], which are obtained based on the traction-compression tests of two cycles. Parallelly, another group of parameters only with isotropic hardening is fitted based on the experimental traction curve in the first cycle. The elastic properties are adopted from Muransky *et al*. [11].

Based on the inactive element method, the following two sections will focus on the effect of kinematic hardening on results at mid-construction and end of the process.

6.1. During the process

As described above, Isotropic hardening and mixed isotropic-kinematic hardening are applied for the process simulation. **Figure 5** shows the comparison, in terms of predicted distortion and stress fields, between two different material laws. The results are demonstrated at the instant close to half of the deposition of the 15th layer, at the mid-construction of the part. It can be shown that the effect of kinematic hardening on the distortion u_t is quite limited, while the stress distribution of σ_{tt} is different for the substrate and the constructed wall.

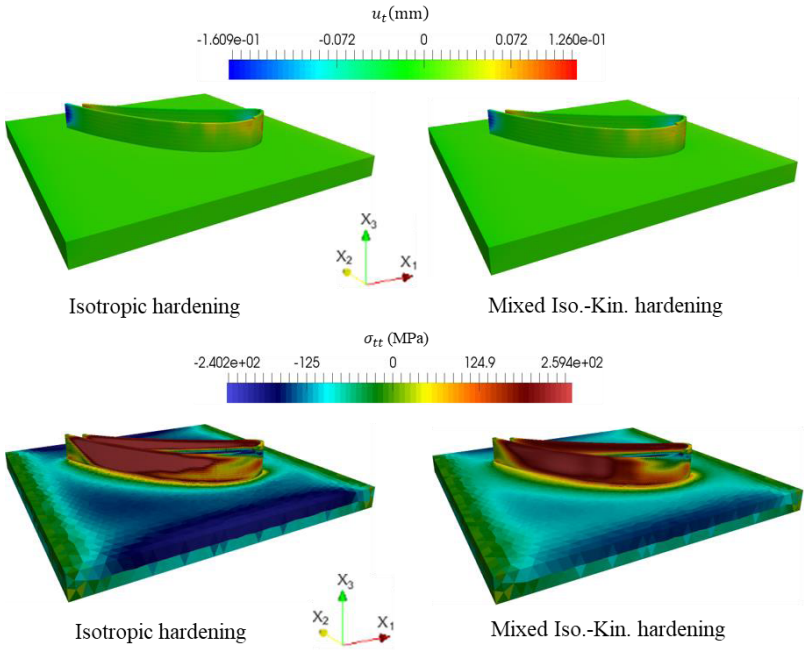

Figure 5.Comparison between isotropic hardening and mixed isotropic-kinematic (Mixed Iso.-Kin.) simulations: displacement field and stress field. The comparison is shown at about half the deposition of the 15th layer.

6.2. End of Construction

After the dwell time of the final construction of the 30th layer, the distortion and stress distributions are given in **Figure 6**. Like those observed at the mid-construction of the 15th layer, the influence of kinematic hardening on the σ_{tt} is obvious. While for the distortion distribution, the influence is not significant.

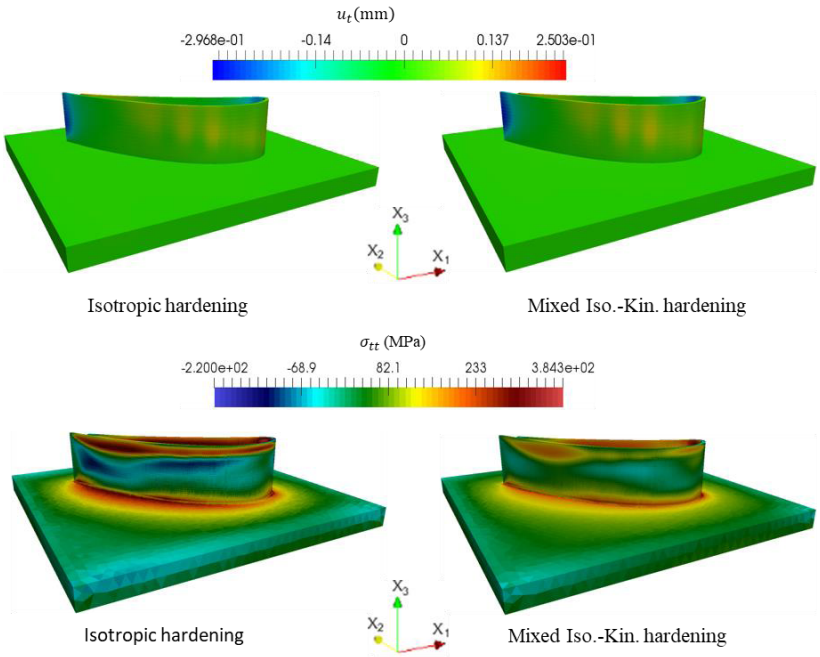

Figure 6. Comparison between isotropic hardening and mixed isotropic-kinematic (Mixed Iso.-Kin.) simulations: displacement field and stress field. The comparison is shown at the final deposition of the 30th layer.

By the above studies on the mid-construction and final construction, the kinematic hardening shows a significant influence on the stress distribution by present studies, while the effect on the distortion is quite limited.

7. Conclusion

In this paper, a thermo-mechanical finite element simulation is developed for additive manufacturing by directed energy deposition (DED). The simulation is conducted at the scale of the part, by modelling the progressive deposition by the way of the fraction of layer, where a group of elements is activated at the same time based on the method of inactive element method. To resolve the problem of discontinuities at the interface between active and inactive elements, a minimization of the quantity of the initial distortions and strains in the inactive domain is proposed. The comparison between the inactive element method and the quiet element method on displacement and stress distribution is discussed. In addition, another important discussion of the effect of kinematic hardening included in the material constitutive on DED process simulation is performed. All the discussions are presented for the mid-construction and the end of construction.

By the comparison of displacement and stress distributions between the inactive element method and the quiet element method, it is found that the inactive element method gives more reasonable results for the distortion prediction, and the stress distribution of the quiet element method with a set of small Young's modulus (1 GPa) in the non-construction domain is like those of the inactive element method.

The kinematic hardening shows a significant influence on the stress distribution, while its effect on the displacement distribution is slight.

By the above studies, the minimization method of the non-construction domain produces less uncertainty compared with the quiet element method. The kinematic hardening is necessary to be considered for the back-and-forth deposition mode of additive manufacturing.

Acknowledgments
The authors wish to acknowledge the financial support from the doctoral school of Mines Paris for the project of **AM-Multi**.

8. References

[1] Wilson J M, Piya C, Shin Y C, Zhao F and Ramani K 2014 *J. Clean. Prod.* **80** 170
[2] Michaleris P 2014. *Finite Elem. Anal. Des.* **86** 51
[3] Biegler M, Marko A, Graf B, Rethmeier M 2018 *Addit. Manuf.* **24** 264
[4] Baiges J, Chiumenti M, Moreira C A, Cervera M and Codina R 2021 *Addit. Manuf.* **37** 101650
[5] Zhang Y, Chen Q, Guillemot G, Gandin C A, Bellet M 2018 *C. R. Mecanique* **346** 1055
[6] Stender M E, Beghini L L, Sugar J D, Veilleux M G, Subia S R, Smith T R, San Marchi C W, Brown A A and Dagel D J 2018 *Addit. Manuf.* **21** 556
[7] Smith M C, Muransky O, Austin C, Bendeich P and Xiong Q 2018 *Int. J. Press. Vessel. Pip. INT J PRES VES PIP* **164** 93
[8] Kim C S 1975 *Technical Report Argonne National Laboratory*, Ill., USA
[9] Keumo Tematio J 2022 *PhD Thesis*, PSL University, Mines Paris
[10] Depradeux L 2004 *Ph.D. Thesis*, INSA Lyon
[11] Muransky O, Smith MC, Bendeich PJ, Edwards L 2011 *Comp. Mater. Sci.* **50** 2203